

# Luminosities and Space Densities of Gamma-Ray Bursts

Maarten Schmidt

*California Institute of Technology, Pasadena, CA 91125*

mxs@deimos.caltech.edu

## ABSTRACT

We use a homogeneous sample of gamma-ray bursts (GRB) extracted from 5.9 years of BATSE DISCLA data (Schmidt 1999) and a variety of assumed broken power-law luminosity functions to derive GRB luminosities and space densities. Luminosity functions that are narrow or exhibit no density evolution produce expected redshift distributions that are incompatible with the observation of a GRB redshift of 3.4. For  $q_o = 0.1$  and density evolution rising to 10 at  $z = 1$ , we find for a variety of slopes of the luminosity function values of the local space density around  $0.18 \text{ Gpc}^{-3} \text{ y}^{-1}$  with a range of only 40%. Characteristic 50 – 300 keV peak luminosities exhibit a range of a factor of 6 around  $6 \times 10^{51} \text{ erg s}^{-1}$ , corresponding to a characteristic total luminosity of  $1.2 \times 10^{53} \text{ erg}$  in the 10 – 1000 keV band. For  $q_o = 0.5$ , densities are higher and luminosities lower, both by a factor of 2.5. The local emissivity of GRBs is  $1.0 \times 10^{52} \text{ erg Gpc}^{-3} \text{ y}^{-1}$  in the 10 – 1000 keV band.

*Subject headings:* cosmology: observations — gamma rays: bursts

## 1. Introduction

Soon after the launch of the *Compton Gamma Ray Observatory* in 1991, observations of gamma-ray bursts (GRB) with the Burst and Transient Source Experiment (BATSE) established two important global properties of GRBs: an isotropic sky distribution (Meegan et al. 1992a) and a radial distribution incompatible with a uniform population in euclidean space (Meegan et al. 1992b). The evidence for a non-uniform radial distribution was based on either the  $N(> P)$  distribution or the  $V/V_{max}$  distribution of the observed GRBs. The  $N(> P)$  distribution of the peak flux  $P$  should be a power law of slope  $-3/2$  for a uniform population in euclidean space. The observed distribution was shallower, particularly at lower fluxes (Meegan et al. 1992a). For a uniform population, the  $V/V_{max}$  distribution would be uniform between 0 and 1, with  $\langle V/V_{max} \rangle = 0.5$  (Schmidt, Higdon and Hueter 1988). Early BATSE observations yielded  $\langle V/V_{max} \rangle = 0.35$ , significantly different from the value expected for homogeneity (Meegan et al. 1992b).

A cosmological distance scale of GRBs is compatible with the isotropic sky distribution and the radial distribution (Paczynski 1992). This has been confirmed by the first observation of a large

redshift for a GRB afterglow (Metzger et al. 1997). The distance scale in this cosmological scenario for GRBs has been derived from the observed  $N(> P)$  distribution, usually on the assumption that GRBs are standard candles (Pendleton et al. 1996; Wijers et al. 1998; Totani 1999). Krumholz, Thorsett, and Harrison (1998) have shown that relaxing the standard candle assumption renders a broad range of models consistent with the BATSE  $N(> P)$  relation.

In this *Letter*, we are reporting the results of setting the cosmological distance scale of GRBs, assuming a full luminosity function and using the euclidean  $\langle V/V_{max} \rangle$  value as a distance indicator. We use the BD2 sample of GRBs derived from 5.9 years of BATSE DISCLA data, briefly described in Sec. 2. The characterization of the luminosity function and its evolution, and the derivation of predicted distributions of luminosity,  $V/V_{max}$ , redshift, and flux are discussed in Sec. 3. The results for a variety of luminosity functions are presented in Sec. 4 and the conclusions are summarized in Sec. 5. We are assuming in this paper a Hubble constant  $H_o = 70 \text{ km s}^{-1} \text{ Mpc}^{-1}$  and zero cosmological constant.

## 2. The BD2 Sample of Gamma-Ray Bursts

We use a large homogeneous sample (the BD2 sample) of 1391 GRBs derived from BATSE DISCLA data, consisting of the continuous data stream from the eight BATSE detectors in four energy channels on a time scale of 1024 msec (Fishman et al. 1989). This sample is a revision, described below, of the BD1 sample which resulted from a search of DISCLA data over the period TJD 8365 – 10528 (Schmidt 1999). The BD1 sample was based on a trigger algorithm that used the background both before and after the onset of the burst and required an excess of at least  $5\sigma$  over background in at least two detectors in the energy range 50 – 300 keV.

In the process of classifying triggers for the creation of the BD1 sample (Schmidt 1999), we had accepted 1018 DISCLA triggers that were within 230 sec of a GRB in the BATSE catalog (Meegan et al. 1999) as genuine GRBs. In addition, we classified another 404 DISCLA triggers as GRBs. In a subsequent revision, we have now inspected the output of the BATSE detectors over a time interval of 12,000 sec around each of the 404 GRBs not in the BATSE catalog, as well as those in the catalog for which times or positions differed appreciably. In the process, we rejected 7 triggers as caused by source fluctuations, 18 turned out to be parts of other GRBs of long duration, and 6 were identified as the soft repeater SGR1806-20 and rejected. As a consequence of the revision, the BD2 sample now contains 1391 GRBs, of which 1013 are listed in the BATSE catalog, another 377 are classified as GRBs, and one as a probable GRB.

For the purpose of this paper, we can characterize the BD2 sample as follows. The number of GRBs is 1391. The sample effectively represents 2.003 years of full sky coverage (Schmidt 1999), so the rate is 694 GRBs per year. The average euclidean  $V/V_{max}$  is  $0.334 \pm 0.008$ . The limiting flux has a distribution  $G(P_{lim})$  that has been derived as follows. For 104 positions of fixed celestial coordinates distributed isotropically around the sky, we checked every 100 sec during every tenth

day whether the sky position was above the horizon and whether the time did not fall in an exclusion window set up to avoid interference or bad data (Schmidt 1999). If so, we converted the limiting count of 5 times the square root of the observed background in the second brightest illuminated detector into a limiting flux  $P_{lim}$ . The resulting distribution  $G(P_{lim})$  has a median at  $0.37 \text{ ph cm}^{-2} \text{ s}^{-1}$ , and 10 and 90 percentiles at  $0.29 \text{ ph cm}^{-2} \text{ s}^{-1}$  and  $0.51 \text{ ph cm}^{-2} \text{ s}^{-1}$ , respectively, in the 50 – 300 keV band.

### 3. Derivation of the Distance Scale

Since the number of redshifts of GRBs is as yet too small for a statistical derivation of the luminosity function, we will instead *assume* a full luminosity function and then use the observed number of GRBs and their euclidean  $\langle V/V_{max} \rangle$  in the BD2 sample to derive properties such as the local space density and the characteristic luminosity  $L^*$ . We will find that these properties vary relatively little as we change the shape of the luminosity function.

#### 3.1. The Luminosity Function

Experience has shown that the differential luminosity function of many types of extragalactic objects can be represented as a broken power law (cf. e.g. Hasinger (1998) for X-ray active galactic nuclei). We will use a broken power law, and in addition introduce upper and lower limits of luminosity, thus allowing both narrow (standard candle) and more realistic broad luminosity functions. We will also assume density evolution, to be introduced below.

The local luminosity function of peak GRB luminosities  $L$ , defined as the co-moving space density of GRBs in the interval  $\log L$  to  $\log L + d \log L$ , is

$$\Phi_o(L) = 0, \quad \text{for} \quad \log L < \log L^* - \Delta_1, \quad (1a)$$

$$\Phi_o(L) = c_o(L/L^*)^{\alpha_1}, \quad \text{for} \quad \log L^* - \Delta_1 < \log L < \log L^*, \quad (1b)$$

$$\Phi_o(L) = c_o(L/L^*)^{\alpha_2}, \quad \text{for} \quad \log L^* < \log L < \log L^* + \Delta_2, \quad (1c)$$

$$\Phi_o(L) = 0, \quad \text{for} \quad \log L > \log L^* + \Delta_2. \quad (1d)$$

Given that most types of extragalactic objects show evolution, and considering that the rate of star formation may be relevant for GRBs (Madau, Pozetti, and Dickinson 1998), we introduce density evolution  $\rho(z)$ . In most cases, we have assumed

$$\rho(z) = (1+z)^p, \quad \text{for} \quad 0 < z < z_p, \quad (2)$$

$$\rho(z) = (1+z_p)^p, \quad \text{for} \quad z > z_p. \quad (3)$$

While any type of evolution can be explored (Che, Yang, and Nemiroff 1999), we have used in this

Letter only the case  $z_p = 1.0$  and  $\rho(1.0) = 10$  without a decline toward larger redshifts (Steidel et al. 1999). The luminosity function at redshift  $z$  is  $\Phi_z(L) = \Phi_o(L)\rho(z)$ .

### 3.2. Predicting the Sample Properties from the Luminosity Function

In principle, with the full characterization of the BD2 sample given in Sec. 2 and the luminosity function  $\Phi_z(L)$  with all its free parameters set, we can predict or model all properties of the sample. Our procedure will be to assume values for the parameters  $\Delta_1$ ,  $\Delta_2$ ,  $\alpha_1$ , and  $\alpha_2$ , and then to vary  $L^*$  until the predicted value of the euclidean  $\langle V/V_{max} \rangle$  equals the observed value in the BD2 sample, and to set  $c_o$  to fit the observed number of GRBs.

The modeling procedure involves the derivation of the peak flux  $P(L, z)$  of a GRB of peak luminosity  $L$  observed at redshift  $z$  (Schmidt and Green 1986),

$$P(L, z) = \frac{L}{4\pi A^2(z)} \frac{C(E_1(1+z), E_2(1+z))}{C(E_1, E_2)} \quad (4)$$

where  $A(z)$  is the bolometric luminosity distance and  $C(E_1, E_2)$  is the integral of the spectral energy distribution between  $E_1 = 50$  keV and  $E_2 = 300$  keV. We use a Band spectrum (Band et al. 1993) for the energy distribution with  $\alpha = -1.0$ ,  $\beta = -2.0$ , and  $E_o = 200$  keV in the restframe.

Objects with luminosity  $L$  observed in a part of the BD2 sample with flux limit  $P_{lim}$  are detectable to a maximum redshift  $z_{max}(L, P_{lim})$  that is easily derived from eq.(4). The total number of objects in the sample is

$$N_{BD2} = \int \Phi_o(L) d \log L \int G(P_{lim}) dP_{lim} \int_0^{z_{max}(L, P_{lim})} \rho(z) (dV/dz) dz \quad (5)$$

Based on this model we can derive the distributions of the peak flux  $P$ , the euclidean  $V/V_{max} = (P/P_{lim})^{-3/2}$ , the peak luminosity  $L$ , and the redshift  $z$ . These form the basis for the discussion of results below.

## 4. Results for a Variety of Luminosity Functions

We exhibit in Table 1 numerical results for 18 luminosity function models, nine each for the cases  $q_o = 0.1$  and  $q_o = 0.5$ . All are based on a Hubble constant  $H_o = 70$  km s<sup>-1</sup> Mpc<sup>-1</sup> and zero cosmological constant. Among the nine cases, two have zero density evolution, six have evolution as described in eqs. (2) and (3), and one is an exponential of cosmic time. In the six cases, we explored variations of the extent of the luminosity function below  $L^*$ , as well as of the logarithmic slopes of both parts, cf. Table 1.

As an example, model 14 uses the deceleration parameter  $q_o = 0.1$  and logarithmic slopes of  $-0.5$  and  $-2.0$  for the power law luminosity function, which extends from  $L^*/10$  to  $100 L^*$ . The

model has density evolution  $\rho(z) = (1+z)^{3.32}$  for  $0 < z < 1$  and  $\rho(z) = 10.0$  for  $z > 1$ . Figure 1 shows the relation between the model values of  $\langle V/V_{max} \rangle$  and  $\log L^*$ . The observed value of  $\langle V/V_{max} \rangle = 0.334 \pm 0.008$  corresponds to  $\log L^* = 51.76 \pm 0.08$ , where the error is the formal error corresponding to that in  $\langle V/V_{max} \rangle$ . The value of  $c_o$  is set by the total number of GRBs in the BD2 sample. With the luminosity function of model 14 fully characterized, we can derive the predicted distributions in the BD2 sample of the luminosities, the fluxes, the  $V/V_{max}$  values and the redshifts; the last three are illustrated in Figure 2 together with the luminosity function. Apart from the obvious onset of incompleteness in the observed fluxes, the predicted  $N(> P)$  agrees well with the observed distribution. The model distribution of  $V/V_{max}$  shows fairly good agreement with the observations. The distribution of redshifts is broad, with some redshifts expected as large as 6. The median redshift is 1.5.

Besides the values of  $\log L^*$  and  $c_o$  derived for each model, we show in Table 1 also the local ( $z = 0$ ) space density  $\rho_o$  of GRBs integrated over the full range of luminosities  $L$ , and the probability  $P_{3.4}$  that a GRB in the BD2 sample has a redshift  $z > 3.4$ . This probability is of interest, since one of the first observed GRB redshifts was 3.4 (Kulkarni et al. 1998). For the models with a standard candle luminosity function or with zero evolution (nos. 11 – 13 and 51 – 53), the values of  $P_{3.4}$  are so low that they are inconsistent with the observed redshift of 3.4. Model 53 is similar to the standard candle luminosity models considered by Wijers et al. (1998) and Totani (1999). Wijers et al. (1998) derived a luminosity about 3.5 times larger, and a local density 2.5 times smaller than those given in Table 1, while Totani (1999) found a luminosity similar to our value. The broad luminosity functions considered by Krumholz, Thorsett, and Harrison (1998) cover a range from  $10^{50} - 10^{52}$  erg s<sup>-1</sup>, overlapping with those in models 54 – 58.

We show in Figure 3 a plot of  $\rho_o$  vs.  $L^*$  for all models. There are clear systematics that can be summarized as follows. From  $q_o = 0.1$  to  $q_o = 0.5$  local densities increase and characteristic luminosities decrease, both by a factor of about 2.5. The effect of the density evolution adopted is to decrease local densities by a factor of 15 – 20 and to increase  $L^*$  by a factor of 3. For given cosmology and evolution, local densities range over a factor less than 2 and  $L^*$  over a factor of 6. Given that  $\rho_o$  and  $L^*$  tend to be inversely correlated, we derived for each model  $E_{out}$ , the total peak output of GRBs per unit volume at  $z = 0$ . As shown in Table 1,  $E_{out}$  is remarkably stable at  $5 \times 10^{50}$  erg s<sup>-1</sup>Gpc<sup>-3</sup> y<sup>-1</sup> for the adopted evolution. For zero evolution,  $E_{out}$  is some 5 times larger.

If the gamma radiation of GRBs is beamed or collimated, say over  $4\pi F$  steradians, then all luminosities should be multiplied by  $F$ , and all space densities divided by  $F$ . The total peak output  $E_{out}$  is unaffected by beaming.

## 5. Summary

We have shown that using primarily  $\langle V/V_{max} \rangle$ , we can derive properties of GRBs of useful accuracy. We have used redshift information only in arguing that the observation of a redshift of 3.4 for a GRB is unlikely if the luminosity function is a standard candle, or if the GRB rate does not evolve with redshift. For density evolution rising to a factor of 10 at  $z = 1$  and  $q_o = 0.1$  (for  $q_o = 0.5$ , cf. Table 1), the local space density is  $0.18 \text{ Gpc}^{-3} \text{ y}^{-1}$ , with a range of only 40% among the models considered. Characteristic peak luminosities range over a factor of 6 around  $6 \times 10^{51} \text{ erg s}^{-1}$  in the 50 – 300 keV band.

Luminosities<sup>1</sup> derived in this study are peak luminosities (strictly per 1024 msec), since the detection of GRBs in the BD2 sample is on that time scale. We estimate the *total* energy radiated by GRBs in gamma rays by integrating over the time profile and by extending the spectral range to 10 – 1000 keV. To account for the total energy radiated in the 50 – 300 keV band integrated over the duration of the burst, we consulted data in the BATSE catalog (Meegan et al. 1999). We find that for the 100 – 200 strongest bursts, the ratio of fluence over peak flux is around 9 – 10 s. The ratio of the energy radiated in a band of 10 – 1000 keV over that in the 50 – 300 keV range based on the Band spectrum (Band et al. 1993) with  $\alpha = -1.0$ ,  $\beta = -2.0$ , and  $E_o = 200 \text{ keV}$  is 2.1. We conclude that total luminosities over the 10 – 1000 keV band are 20 times larger than the 50 – 300 keV peak luminosities. Employing this factor, we obtain for  $q_o = 0.1$  a characteristic GRB luminosity of  $1.2 \times 10^{53} \text{ erg}$  in the 10 – 1000 keV band. Similarly, the local emissivity of GRBs  $E_{out}$  discussed in Sec. 4 is  $1.0 \times 10^{52} \text{ erg Gpc}^{-3} \text{ y}^{-1}$  in the 10 – 1000 keV band with very little range among the models.

## REFERENCES

- Band, D. L., et al. 1993, ApJ, 413, 281
- Che, H., Yang, Y., and Nemiroff, R. J. 1999, ApJ, 516, 559
- Fishman, G. J., et al. 1989, GRO Science Workshop Proc., Greenbelt: NASA/GSFC, 2
- Hasinger, G. 1998, Astr. Nachr., 319, 37
- Krumholz, M., Thorsett, S. E., and Harrison, F. A. 1998, ApJ, 506, L81
- Kulkarni, S., et al. 1998, Nature, 393, 35

---

<sup>1</sup>An investigation of the reason why our flux limits  $G(P_{lim})$  (cf. end of Sec. 2) are higher than those given by Pendleton et al. (1998) suggests the possibility that all our fluxes  $P$  may be high by around 27% compared to BATSE fluxes. If this is confirmed, then the values of  $\log L^*$  in Table 1 should be corrected by  $-0.10$  and the emissivities  $E_{out}$  reduced by 27%, while space densities are essentially unchanged.

- Madau, P., Pozzetti, L., and Dickinson, M. E. 1998, *ApJ*, 498, 106
- Meegan, C. A., Fishman, G. J., Wilson, R. B., et al. 1992a, *Nature*, 355, 143
- Meegan, C. A., Fishman, G. J., Wilson, R. B., et al. 1992b, *AIP Conf. Proc.* 265, *Gamma-Ray Bursts*, W. S. Paciesas and G. J. Fishman, New York: AIP, 61
- Meegan, C. A., et al., 1999, <http://www.batse.msfc.nasa.gov/data/grb/catalog>
- Metzger et al., 1997, *Nature*, 387, 878
- Paczynski, B. 1992, *AIP Conf. Proc.* 265, *Gamma-Ray Bursts*, W. S. Paciesas and G. J. Fishman, New York: AIP, 144
- Pendleton, G. N., Mallozzi, R.S., Paciesas, W. S., et al. 1996, *ApJ*, 464, 606
- Pendleton, G. N., Hakkila, J., and Meegan, C.A. 1998, *AIP Conf. Proc.* 428, *Gamma-Ray Bursts*, C.A. Meegan, R. D. Preece, and T. M. Koshut, New York: AIP, 899
- Schmidt, M. 1999, *A&ASuppl.*, 138, No. 3 (Sep 1999 issue) (astro-ph/9908190)
- Schmidt, M., and Green, R. P. 1986, *ApJ*, 305, 68
- Schmidt, M., Higdon, J., and Heuter, G. 1988, *ApJ*, 329, 85
- Steidel, C. C., Adelberger, K. L., Giavalisco, M. et al. 1999, *ApJ*, 519, 1
- Totani, T. 1999, *ApJ*, 511, 41
- Wijers, R. A. M. J., Bloom, J. S., Bagla, J. S., et al., 1998, *MNRAS*, 294, L13

Fig. 1.— Plot of the euclidean value of  $\langle V/V_{max} \rangle$  versus peak luminosity for luminosity function model 14, cf. Table 1.

Fig. 2.— Properties of luminosity function model 14, cf. Table 1. Panel (a) shows the luminosity function  $\Phi(L)$  ( $\text{Gpc}^{-3} \text{y}^{-1}$  per unit  $\log L$ ). The break luminosity  $L^*$  has been set by  $V/V_{max}$  and the normalization by the observed rate of GRBs. Panel (b) compares the model euclidean  $V/V_{max}$  distribution for the BD2 sample with the observed distribution. Panel (c) compares the model flux distribution  $N(> P)$  for the BD2 sample with the observations. Panel (d) shows the expected distribution of redshifts for the BD2 sample, with an indication of the probability  $P_{3.4}$  of a redshift exceeding 3.4.

Fig. 3.— Plot of the local GRB density versus peak luminosity  $L^*$  for 18 luminosity function models, cf. Table 1. The systematic effects of the cosmological model ( $q_o = 0.1$  and  $q_o = 0.5$ ) and of evolution are easily discerned. For a given cosmological model and evolution, local densities range over a factor of 2, and luminosities over a factor of 6 for the different luminosity function models considered.



Table 1. Properties of various luminosity functions models.

#	$q_o^a$	$p$	$z_p$	$\Delta_1$	$\Delta_2$	$\alpha_1$	$\alpha_2$	$\log L^{*b}$	$c_o^c$	$\rho_o^d$	$P_{3.4}^e$	$E_{out}^f$
11	0.1	0.00	0.0	-0.1	0.1	-0.5	-2.0	51.11	10.2	2.0	0%	26.1
12	0.1	0.00	0.0	-1.0	2.0	-0.5	-2.0	51.34	1.30	2.7	1%	29.0
13	0.1	3.32	1.0	-0.1	0.1	-0.5	-2.0	51.44	0.654	0.13	0%	3.6
14	0.1	3.32	1.0	-1.0	2.0	-0.5	-2.0	51.76	0.0740	0.15	5%	4.4
15	0.1	3.32	1.0	-2.0	2.0	-0.5	-2.0	52.20	0.0276	0.22	13%	5.3
16	0.1	3.32	1.0	-1.0	2.0	0.0	-2.0	51.62	0.128	0.16	5%	4.3
17	0.1	3.32	1.0	-1.0	2.0	-1.0	-2.0	51.92	0.0364	0.15	5%	4.3
18	0.1	3.32	1.0	-1.0	2.0	-0.5	-1.0	51.43	0.0842	0.19	14%	5.8
19	0.1	4.04 <sup>g</sup>	1.0	-1.0	2.0	-0.5	-2.0	51.72	0.0780	0.16	5%	4.2
51	0.5	0.00	0.0	-0.1	0.1	-0.5	-2.0	50.71	25.0	5.0	0%	25.7
52	0.5	0.00	0.0	-1.0	2.0	-0.5	-2.0	50.96	3.18	6.6	1%	29.6
53	0.5	3.32	1.0	-0.1	0.1	-0.5	-2.0	51.08	1.66	0.33	0%	4.0
54	0.5	3.32	1.0	-1.0	2.0	-0.5	-2.0	51.42	0.189	0.39	5%	5.0
55	0.5	3.32	1.0	-2.0	2.0	-0.5	-2.0	51.77	0.0857	0.69	9%	6.1
56	0.5	3.32	1.0	-1.0	2.0	0.0	-2.0	51.26	0.334	0.40	4%	4.9
57	0.5	3.32	1.0	-1.0	2.0	-1.0	-2.0	51.57	0.0927	0.38	5%	5.0
58	0.5	3.32	1.0	-1.0	2.0	-0.5	-1.0	51.06	0.234	0.54	11%	7.0
59	0.5	3.56 <sup>g</sup>	1.0	-1.0	2.0	-0.5	-2.0	51.34	0.205	0.43	4%	4.6

<sup>a</sup>In all cases we use  $H_o = 70 \text{ km s}^{-1} \text{ Mpc}^{-1}$  and zero cosmological constant.

<sup>b</sup> $L^*$  is the peak luminosity in  $\text{erg s}^{-1}$  in the 50 – 300 keV band, if the GRB is radiating isotropically.

<sup>c</sup>Units are  $\text{Gpc}^{-3} \text{ y}^{-1}$  per unit  $\log L$ .

<sup>d</sup> $\rho_o$  is the local ( $z = 0$ ) GRB rate, in units of  $\text{Gpc}^{-3} \text{ y}^{-1}$ .

<sup>e</sup>Probability of  $z > 3.4$  for a GRB in the BD2 sample.

<sup>f</sup>Local peak energy output of GRBs in the 50 – 300 keV band, in units of  $10^{50} \text{ erg s}^{-1} \text{ Gpc}^{-3} \text{ y}^{-1}$ .

<sup>g</sup>In this case  $\rho(z) = e^{p\tau(z)}$  where  $\tau(z)$  is the light travel time, expressed in the age of the universe.

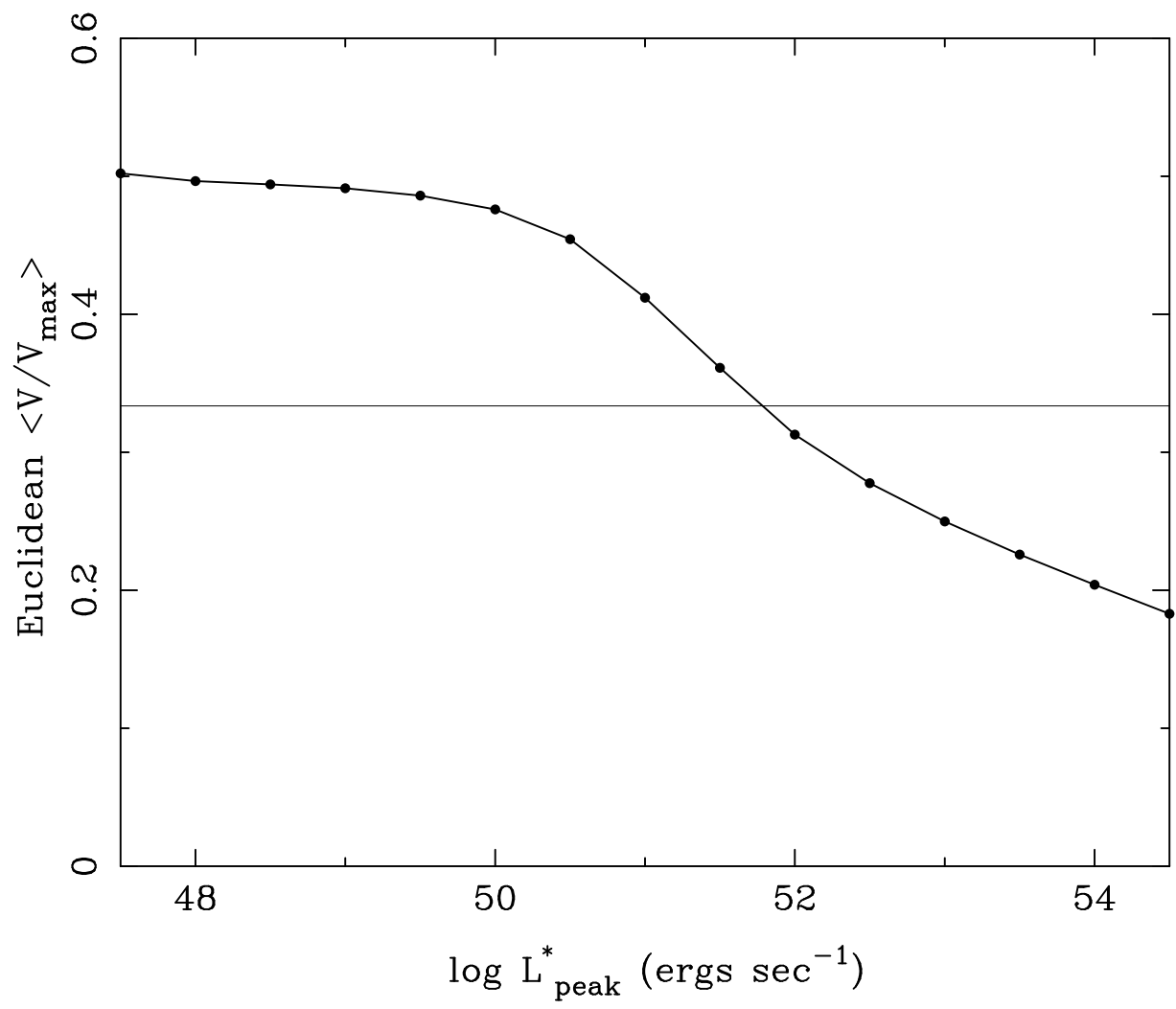


*Figure 1*

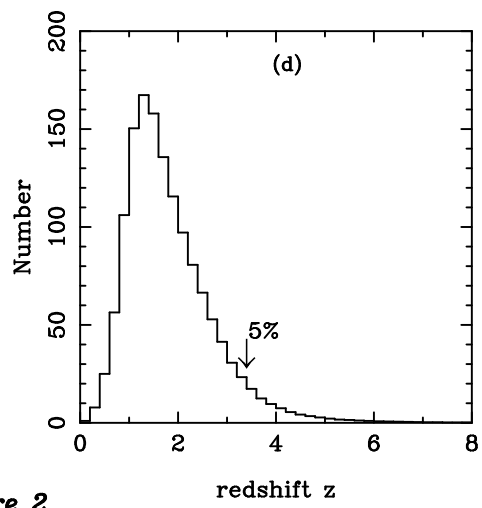
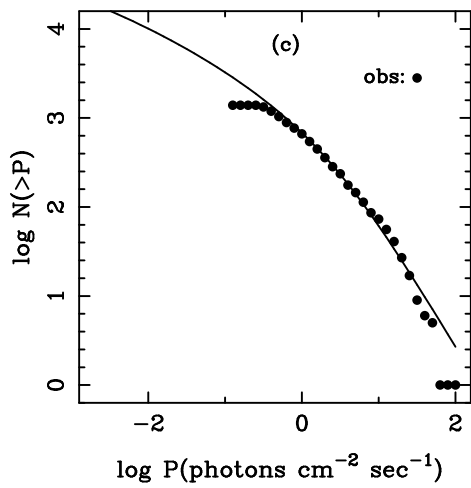
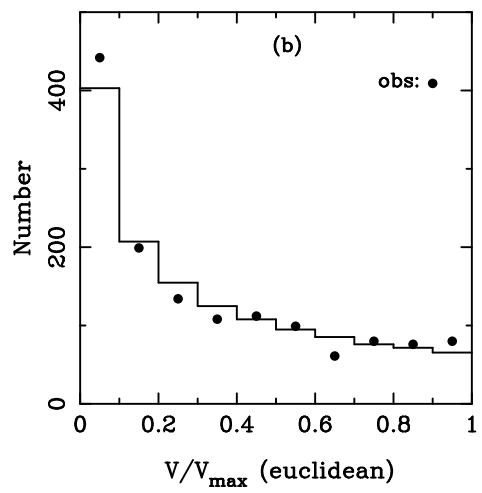
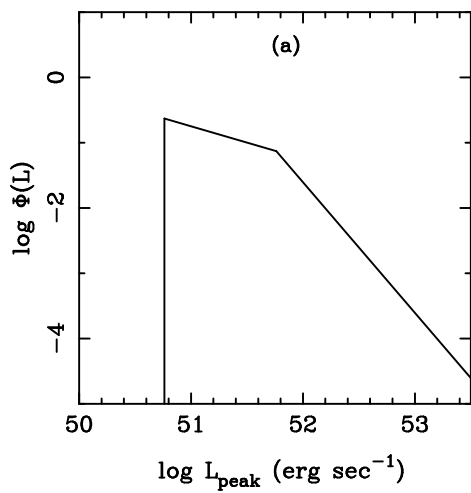
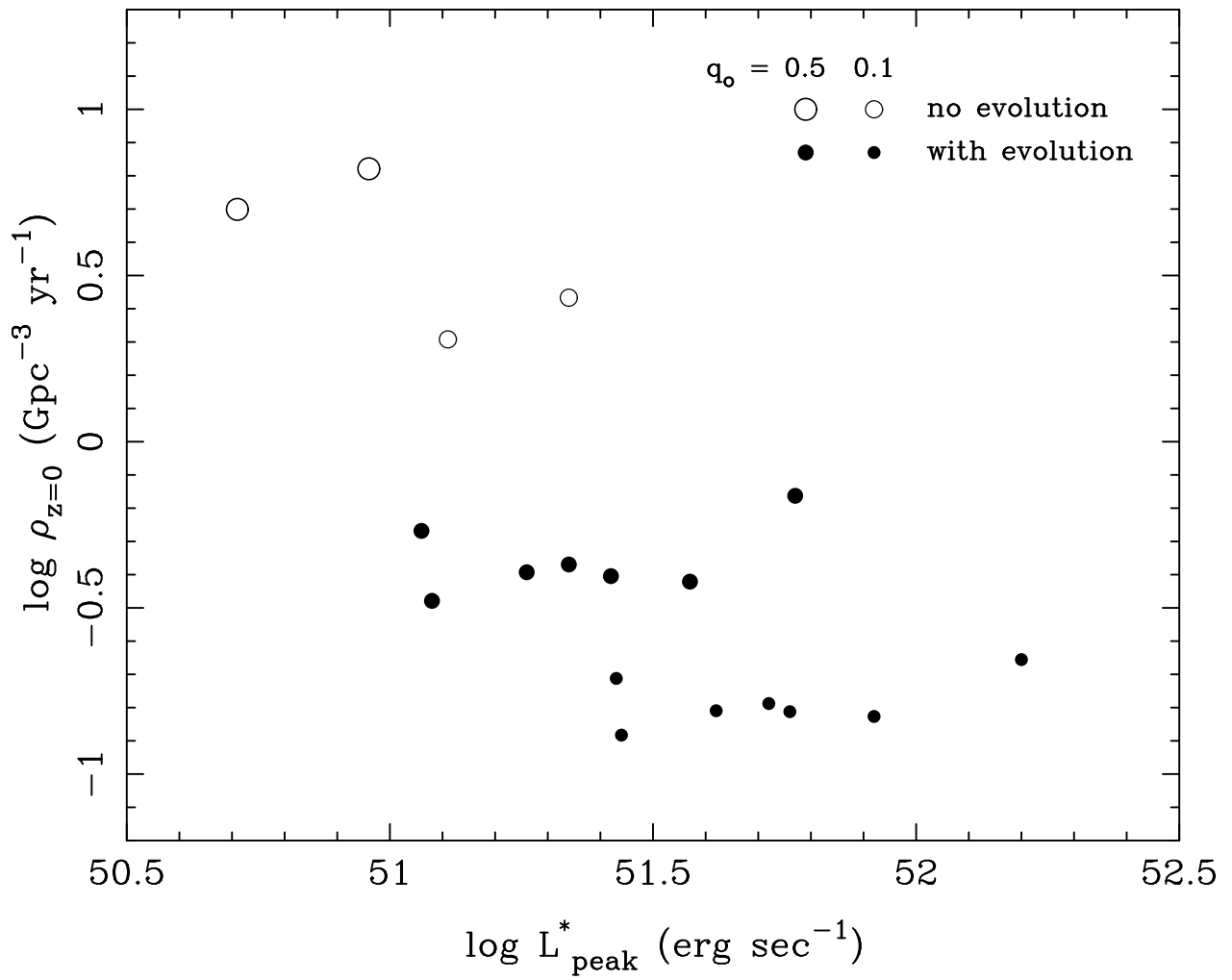


Figure 2



*Figure 3*